



Contents lists available at ScienceDirect

Journal of Sound and Vibration

journal homepage: www.elsevier.com/locate/jsv

A simple formula for predicting resonant frequencies of a rectangular plate with uniformly restrained edges

K.M. Li*, Z. Yu

Ray W. Herrick Laboratories, School of Mechanical Engineering, Purdue University, 140 S. Martin Jischke Drive, West Lafayette, IN 47907-2031, USA

ARTICLE INFO

Article history:

Received 28 March 2009

Received in revised form

31 May 2009

Accepted 10 June 2009

Handling Editor: M.P. Cartmell

Available online 17 July 2009

ABSTRACT

This paper provides empirical formulas for rapidly calculating the resonant frequencies of an orthotropic, rectangular plate with its edges constrained by elastic supports. In particular, the classical boundary condition with guided supports at its edges is considered. Other boundary conditions, such as the guided–free edges, guided–clamped edges and guided–free support edges have also been included in the present study. Simple and closed form empirical formulas have been derived to allow straightforward computations of the modal resonant frequencies. The empirical formulas are based on the analytical results obtained from the Rayleigh–Ritz method. However, the coefficient is determined empirically from the results obtained by other more accurate computational scheme, e.g. finite element method. The method is further generalized to predict the resonant frequencies for general boundary conditions of a square, orthotropic plate.

© 2009 Elsevier Ltd. All rights reserved.

1. Introduction

The study of flexural vibration of a rectangular plate has been a subject of extensive research for a few decades [1–27]. The determination of natural frequencies is often the focus of these studies because the plate's responses due to external excitations are usually dominated by the resonant responses. Leissa [6,7] presented a comprehensive review for calculating the resonant frequencies of rectangular plates supported at their edges with the classical boundary conditions.

Use of Rayleigh's method, Warburton [3,4] applied characteristic beam vibration functions (see, for example Ref. [25]) to develop a simple approximate expression to calculate the resonant frequencies for the flexural vibration of thin, isotropic, rectangular plates having any combination of clamped, free or simply supported edges with an arbitrary aspect ratio. Warburton [3] arranged the solutions for six classical boundary conditions in a tabular form for ease of reference. Dickinson [8] subsequently generalized Warburton's method to give the corresponding approximate expressions for orthotropic, rectangular plates with the results for isotropic plates as a particular case. These expressions [25] for calculating the resonant frequencies are straightforward and no prior knowledge of vibration theory are needed.

It is also remarkable that the three general boundary conditions (free, simply supported and clamped edges) are commonly considered in the early studies. However, these classical boundary conditions are never fully achieved in reality. It is understood that the support along the plate's edges is always elastic in nature. More importantly, it is not only convenient but also necessary to rapidly calculate the natural frequencies of rectangular panels for a quick check on the resonant responses during the design stage of many engineering problems. To meet this purpose, Nassar [15] developed a simple analytical formula to approximate the resonant frequencies of a translationally restrained isotropic, rectangular

* Corresponding author. Tel.: +1 765 494 1099; fax: +1 765 494 0787.

E-mail address: mmkml@purdue.edu (K.M. Li).

plate where the rotational stiffness along the edges is allowed to vary. Gorman [16–18] used a superposition method to calculate numerically the natural frequencies of the isotropic/orthotropic, rectangular plates with different classical boundary conditions at the edges. However, there are usually no exact solutions when the edges of the plates are supported with general elastic constants.

The objectives of the current paper are twofold. First, we wish to develop approximate formulas to calculate the resonant frequencies for rectangular plates with guided (also referred as sliding) edges. Although the occurrence of guided supported for a panel is less frequently met in engineering applications, it is useful to document such formulas for future reference. To this end, we start our analysis by deriving a set of non-dimensional governing equations for determining the transverse vibration of orthotropic plates. From the non-dimensional analysis, we show that the approximate formulas for the resonant frequencies of the four general boundary conditions have the same form. They can be expressed in terms of the geometric ratio, the stiffness ratio and Poisson’s ratio. In addition, the natural frequencies also vary with constant coefficients which are dependent on the types of support (free, simply supported, clamped and guided) at the edges. To simplify the analysis, we assume that the supports are uniform and the same as the adjacent edges although the opposite edges may have different elastic constants. Secondly, we aim to develop empirical formulas for the natural frequencies of a square, orthotropic plate with an arbitrary elastic constant: either the translational stiffness or rotational stiffness is allowed to vary.

In the current study, we examine a more general situation: the flexural vibration of the orthotropic plates. It is because many engineering structures are made of composite materials which may be modelled conveniently as orthotropic, rectangular plates. Furthermore, panels with unequal stiffening along two orthogonal directions, such panels as walls and ceilings used in the building structures are often modelled as the orthotropic plates.

To the best of our knowledge, the formulas developed here are not found in the previous literature. They serve as a convenient tool for calculating the natural frequencies of the transverse vibration of the orthotropic/isotropic plates. In addition, the methodology can easily be applied in other situations to calculate the resonant frequencies for plates with different elastic constants.

2. Formulation of the problem

A thin elastic plate, which has uniform thickness h and mass per unit area S_ρ , is aligned in the x - y plane with $x \in (0, L_x)$ and $y \in (0, L_y)$. Suppose that the edges of the rectangular plate are uniformly restrained with linear elastic springs. We assume a more general situation where the rectangular plate is made of orthotropic materials since an isotropic plate can be treated as a special case. Fig. 1 shows the schematic diagram of the problem.

For an orthotropic plate restraining uniformly along its edges, the governing equation for its transverse displacement, $w(x, y)$, is given by [26,27]

$$B_x \frac{\partial^4 w}{\partial x^4} + 2(B_{xy} + 2B_k) \frac{\partial^4 w}{\partial x^2 \partial y^2} + B_y \frac{\partial^4 w}{\partial y^4} - S_\rho \omega^2 w = 0, \tag{1}$$

where ω is the angular frequency of the vibration, the four orthotropic constants are defined as follows:

$$B_x = E_x h^3 / 12(1 - \nu_x \nu_y), \tag{2a}$$

$$B_y = E_y h^3 / 12(1 - \nu_x \nu_y), \tag{2b}$$

$$B_{xy} = \nu_x B_y = \nu_y B_x \tag{2c}$$

and

$$B_k = G_k h^3 / 12, \tag{2d}$$

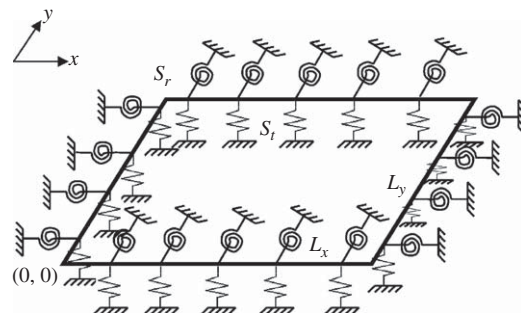


Fig. 1. Geometric configuration of an elastically restrained rectangular plate.

where E_x and E_y are the respective Young’s moduli, ν_x and ν_y are the respective Poisson’s ratios in the x - and y -directions and G_k is the shear modulus of the orthotropic plate. Use of a symmetric argument of the orthotropic plate leads to the identity of $\nu_x E_y = \nu_y E_x$. Hence, B_{xy} can be written in the form given in Eq. (2c).

To facilitate the subsequent analysis, it is useful to express the governing differential equation in a non-dimensional form as

$$\bar{B}_x \frac{\partial^4 \bar{w}}{\partial \bar{x}^4} + 2(\bar{B}_{xy} + 2\bar{B}_k) \frac{\partial^4 \bar{w}}{\partial \bar{x}^2 \partial \bar{y}^2} + \bar{B}_y \frac{\partial^4 \bar{w}}{\partial \bar{y}^4} - \bar{\omega}^2 \bar{w} = 0, \tag{3}$$

where overbar represents the corresponding parameter in its non-dimensional form. The flexural displacement, $w(x, y)$ is non-dimensionalized by h , the width (measured in the x -direction) by L_x and the length (measured in the y -direction) by L_y , the four orthotropic constants are non-dimensionalized by B_m and the angular frequency of the vibration, ω is non-dimensionalized by

$$\omega_s = \sqrt{B_m/S\rho}/L_x L_y, \tag{4}$$

where B_m is the geometric mean of the direct bending stiffness in the x - and y -directions, i.e.

$$B_m = \sqrt{B_x B_y} = E_m h^3 / 12(1 - \nu_m^2), \tag{5a}$$

E_m and ν_m are the geometric means of Young’s moduli and Poisson’s ratios, respectively. They are defined as follows:

$$E_m = \sqrt{E_x E_y} \tag{5b}$$

and

$$\nu_m = \sqrt{\nu_x \nu_y}. \tag{5c}$$

By using Eqs. (2a)–(2d) and (5a)–(5c), we can show that the four non-dimensional orthotropic constants can be reduced to

$$\bar{B}_x = B_x/B_m = \sqrt{E_x/E_y}, \tag{6a}$$

$$\bar{B}_y = B_y/B_m = \sqrt{E_y/E_x}, \tag{6b}$$

$$\bar{B}_{xy} = B_{xy}/B_m = \nu_m \tag{6c}$$

and

$$\bar{B}_k = B_k/B_m = G_k(1 - \nu_m^2)/E_m. \tag{6d}$$

Substitution of Eqs. (6a)–(6d) into Eq. (3) leads to an expression for the non-dimensional governing equation:

$$\sqrt{\frac{E_x}{E_y}} \frac{\partial^4 \bar{w}}{\partial \bar{x}^4} + 2 \left[\nu_m + \frac{2G_k(1 - \nu_m^2)}{E_m} \right] \frac{\partial^4 \bar{w}}{\partial \bar{x}^2 \partial \bar{y}^2} + \sqrt{\frac{E_y}{E_x}} \frac{\partial^4 \bar{w}}{\partial \bar{y}^4} - \bar{\omega}^2 \bar{w} = 0 \tag{7}$$

which is independent on the four non-dimensional orthotropic constants.

The bending and twisting moments per unit length can be expressed in terms of w as follows:

$$\begin{bmatrix} M_x \\ M_y \\ M_{xy} \end{bmatrix} = - \begin{bmatrix} B_x & B_{xy} & 0 \\ B_{xy} & B_y & 0 \\ 0 & 0 & B_k \end{bmatrix} \begin{bmatrix} \partial^2 w / \partial x^2 \\ \partial^2 w / \partial y^2 \\ 2\partial^2 w / \partial x \partial y \end{bmatrix} \tag{8}$$

and the shear forces per unit length in the x - and y -directions can be written as

$$Q_x = \frac{\partial M_x}{\partial x} + \frac{\partial M_{xy}}{\partial y} = -B_x \frac{\partial^3 w}{\partial x^3} - (B_{xy} + 2B_k) \frac{\partial^3 w}{\partial x \partial y^2}, \tag{9a}$$

$$Q_y = \frac{\partial M_y}{\partial y} + \frac{\partial M_{xy}}{\partial x} = -B_y \frac{\partial^3 w}{\partial y^3} - (B_{xy} + 2B_k) \frac{\partial^3 w}{\partial x^2 \partial y}. \tag{9b}$$

For uniformly restrained edges, the boundary conditions for the rectangular orthotropic plate are given by

$$S_{t,1} w = Q_x, \quad S_{r,1} \partial w / \partial x = -M_x, \quad \text{at } x = 0; \tag{10a,b}$$

$$S_{t,2} w = -Q_y, \quad S_{r,2} \partial w / \partial y = M_y, \quad \text{at } y = L_y; \tag{10c,d}$$

$$S_{t,3} w = -Q_x, \quad S_{r,3} \partial w / \partial x = M_x, \quad \text{at } x = L_x; \tag{10e,f}$$

$$S_{t,4} w = Q_y, \quad S_{r,4} \partial w / \partial x = -M_y, \quad \text{at } y = 0; \tag{10g,h}$$

where S_t and S_r are the translational and rotational stiffness per unit length. The subscripts 1, 2, 3 and 4 represent the physical properties of the four edges counting clockwise from the left vertical edge at $x = 0$.

A set of non-dimensionalized boundary conditions for the problem can then be obtained by substituting Eqs. (8), (9a) and (9b) into Eqs. (10a)–(10h) to yield

$$\bar{S}_{t,1}\bar{w} = -R^{-1}\sqrt{E_x/E_y}\frac{\partial^3\bar{w}}{\partial\bar{x}^3} - [v_m + 2G_k(1 - v_m^2)/E_m]R\frac{\partial^3\bar{w}}{\partial\bar{x}\partial\bar{y}^2} \quad \text{at } x = 0, \tag{11a}$$

$$\bar{S}_{r,1}\frac{\partial\bar{w}}{\partial\bar{x}} = R^{-1}\sqrt{E_x/E_y}\partial^2\bar{w}/\partial\bar{x}^2 + v_mR\partial^2\bar{w}/\partial\bar{y}^2 \quad \text{at } x = 0, \tag{11b}$$

$$\bar{S}_{t,2}\bar{w} = -R\sqrt{E_y/E_x}\frac{\partial^3\bar{w}}{\partial\bar{y}^3} - [v_m + 2G_k(1 - v_m^2)/E_m]R^{-1}\frac{\partial^3\bar{w}}{\partial\bar{x}\partial\bar{y}^2} \quad \text{at } y = L_y, \tag{11c}$$

$$\bar{S}_{r,2}\frac{\partial\bar{w}}{\partial\bar{x}} = R\sqrt{E_x/E_y}\partial^2\bar{w}/\partial\bar{x}^2 + (v_m/R)\partial^2\bar{w}/\partial\bar{y}^2 \quad \text{at } y = L_y, \tag{11d}$$

$$\bar{S}_{t,3}\bar{w} = R^{-1}\sqrt{E_x/E_y}\frac{\partial^3\bar{w}}{\partial\bar{x}^3} + [v_m + 2G_k(1 - v_m^2)/E_m]R\frac{\partial^3\bar{w}}{\partial\bar{x}\partial\bar{y}^2} \quad \text{at } x = L_x, \tag{11e}$$

$$\bar{S}_{r,3}\frac{\partial\bar{w}}{\partial\bar{x}} = -[R^{-1}\sqrt{E_x/E_y}\partial^2\bar{w}/\partial\bar{x}^2 + v_mR\partial^2\bar{w}/\partial\bar{y}^2] \quad \text{at } x = 0, \tag{11f}$$

$$\bar{S}_{t,4}\bar{w} = R\sqrt{E_y/E_x}\frac{\partial^3\bar{w}}{\partial\bar{y}^3} + [v_m + 2G_k(1 - v_m^2)/E_m]R^{-1}\frac{\partial^3\bar{w}}{\partial\bar{x}\partial\bar{y}^2} \quad \text{at } y = L_y, \tag{11g}$$

$$\bar{S}_{r,4}\frac{\partial\bar{w}}{\partial\bar{x}} = -[R\sqrt{E_x/E_y}\partial^2\bar{w}/\partial\bar{x}^2 + (v_m/R)\partial^2\bar{w}/\partial\bar{y}^2] \quad \text{at } y = L_y, \tag{11h}$$

where R is the aspect ratio of the rectangular plate which is given by

$$R = L_y/L_x. \tag{12}$$

The respective non-dimensional spring constants are defined by

$$\bar{S}_{t,1} = \frac{S_{t,1}L_y}{B_m/L_xL_y}, \tag{13a}$$

$$\bar{S}_{t,3} = \frac{S_{t,3}L_y}{B_m/L_xL_y}, \tag{13b}$$

$$\bar{S}_{r,1} = \frac{S_{r,1}L_y}{B_m}, \tag{13c}$$

$$\bar{S}_{r,3} = \frac{S_{r,3}L_y}{B_m}, \tag{13d}$$

$$\bar{S}_{t,2} = \frac{S_{t,1}L_x}{B_m/L_xL_y}, \tag{13e}$$

$$\bar{S}_{t,4} = \frac{S_{t,4}L_x}{B_m/L_xL_y}, \tag{13f}$$

$$\bar{S}_{r,2} = \frac{S_{r,2}L_x}{B_m}, \tag{13g}$$

$$\bar{S}_{r,4} = \frac{S_{r,4}L_x}{B_m}. \tag{13h}$$

For the special case of an isotropic plate, we have $E = E_m$, $\nu = \nu_m$ and $G_k = E/2(1 + \nu)$. Hence, we can write

$$B_x = B_y = B = Eh^3/12(1 - \nu^2), \tag{14a}$$

$$B_{xy} = Eh^3\nu/12(1 - \nu^2), \tag{14b}$$

$$B_k = Eh^3/24(1 + \nu) \tag{14c}$$

and

$$B_{xy} + 2B_k = B. \quad (14d)$$

With Eqs. (14a)–(14d), the governing differential equations and the associated boundary conditions, cf Eqs. (3) and Eqs. (11a)–(11h) can then be reduced to the identical form given by Li et al. [24]. The non-dimensional spring constants are different for different edges for general boundary conditions. There are no simple analytical and empirical formulas to calculate the resonant frequencies of the rectangular plate with the general boundary conditions. It is possible to use the series solution technique [22–24] to solve for the resonant frequencies of the orthotropic panel. On the other hand, we may use other numerical techniques, e.g. the standard finite element method (FEM) and a systematic superposition method [16–18], to solve Eq. (3) subject to the boundary conditions given in Eqs. (11a)–(11h). However, we endeavour to develop simple empirical solutions for some special cases detailed in the next sections.

3. An empirical formula for the guided support and other classical boundary conditions

It is of interest to note that there is a solution for Eq. (3) if the edges are restrained uniformly for the translation stiffness, S_t and the rotation stiffness, S_r such that

$$S_t = S_{t,1} = S_{t,2} = S_{t,3} = S_{t,4} \quad (15a)$$

and

$$S_r = S_{r,1} = S_{r,2} = S_{r,3} = S_{r,4}. \quad (15b)$$

When the spring constants becomes very small ($S_t = S_r = 0$) or very large ($S_t = S_r \rightarrow \infty$), we can see that the non-dimensional spring constants for all edges become independent on the geometric dimensions of the plate with

$$\bar{S}_t = \bar{S}_{t,1} = \bar{S}_{t,2} = \bar{S}_{t,3} = \bar{S}_{t,4} \quad (16a)$$

and

$$\bar{S}_r = \bar{S}_{r,1} = \bar{S}_{r,2} = \bar{S}_{r,3} = \bar{S}_{r,4}. \quad (16b)$$

In particular, four types of classical boundary conditions can be identified:

- (1) Free edges, denoted by [FFFF], with $\bar{S}_t = \bar{S}_r = 0$.
- (2) Simply supported edges, denoted by [SSSS], with $\bar{S}_t \rightarrow \infty$ and $\bar{S}_r = 0$.
- (3) Clamped edges, denoted by [CCCC], with $\bar{S}_t \rightarrow \infty$ and $\bar{S}_r \rightarrow \infty$.
- (4) Guided edges, denoted by [GGGG], with $\bar{S}_t = 0$ and $\bar{S}_r \rightarrow \infty$.

Based on Warburton's analysis [3], Dickinson and his co-worker [8,9] used the Rayleigh method to obtain an approximate expression for the resonant frequencies of a thin orthotropic plate for the boundary conditions given in (1), (2) and (3) above. The resonant frequencies can be written in a non-dimensional form as

$$\bar{f}_{ij} = \frac{\pi}{2} \sqrt{(Q_i Q_j)^2 (\bar{R}_{ij}^2 + \bar{R}_{ij}^{-2}) + 2\bar{B}_{xy} H_i H_j + 4\bar{B}_{kij} I_j}, \quad (17)$$

where $\bar{f}_{ij}(= \bar{\omega}_{ij}/2\pi)$ is the non-dimensional natural frequency of the mode indices (i, j) and the dimensionless length ratio \bar{R}_{ij} is determined by

$$\bar{R}_{ij} = \frac{(B_x)^{1/4} (Q_i/L_x)}{(B_y)^{1/4} (Q_j/L_y)} = (E_x/E_y)^{1/4} (Q_i/Q_j) R \quad (18)$$

and the aspect ratio, R , is defined in Eq. (12). It is of interest to note that the dimensionless length ratio \bar{R}_{ij} becomes infinite when $Q_j = 0$ and $1/\bar{R}_{ij}$ becomes unbounded when $Q_i = 0$. However, the term $(Q_i Q_j)^2 (\bar{R}_{ij}^2 + \bar{R}_{ij}^{-2})$ remains finite in both situations. Hence, \bar{f}_{ij} is finite and bounded in these two limiting cases, cf Eq. (17).

From the dimensional analysis detailed above, the parameters Q_ε , H_ε and J_ε (for the index $\varepsilon = i$ or j) are constants which only depend on whether \bar{S}_t and/or \bar{S}_r is 0 or ∞ . They can be determined straightforwardly by means of the Rayleigh method for [FFFF], [SSSS] and [CCCC]. For higher order modes (i or j greater than 3), Q_ε , H_ε and J_ε can be expressed conveniently in terms of a set of constants: $\beta_Q(\bar{S}_t, \bar{S}_r)$, $\beta_H(\bar{S}_t, \bar{S}_r)$ and $\beta_J(\bar{S}_t, \bar{S}_r)$ as follows:

$$Q_\varepsilon = \varepsilon + \beta_Q, \quad (19a)$$

$$H_\varepsilon = Q_\varepsilon^2 (1 + \beta_H/Q_\varepsilon) \quad (19b)$$

and

$$J_\varepsilon = Q_\varepsilon^2 (1 + \beta_J/Q_\varepsilon). \quad (19c)$$

For [SSSS], the constants β_Q , β_H and β_J can be determined exactly as

$$\beta_Q = \beta_H = \beta_J = 0. \tag{20a}$$

For [FFFF] and [CCCC], they can be determined approximately [8] to give

$$\beta_Q = -3/2, \quad \beta_H = -2/\pi \quad \text{and} \quad \beta_J = 6/\pi \quad \text{for [FFFF]}, \tag{20b}$$

$$\beta_Q = 1/2, \quad \beta_H = -2/\pi, \quad \text{and} \quad \beta_J = -2/\pi \quad \text{for [CCCC]}. \tag{20c}$$

Table 1 lists these numerical values Q , H and J for i or j less than and equal to 3. Table 1 also gives the functions for β_Q , β_H and β_J for higher order modes.

To confirm the validity of the analytical formula for orthotropic plates, Eq. (17) is used to calculate the resonant frequencies. The computed results are compared with the published results given by Sakata et al. [14]. Their results were presented in term of a non-dimensional factor, $\bar{\lambda}_{ij} = \omega L_x^2 \sqrt{S\rho/Bx}$, which can easily be converted to \bar{f}_{ij} by multiplying the factor of $(R/2\pi)(E_x/E_y)^{1/4}$. Figs. 2 and 3 show, respectively, the comparisons of the resonant frequencies calculated by both methods for simply supported and the clamped plates. The difference between modified Sakata's result and the numerical results according to Eq. (17) is generally well below 1 percent. We also compare the results according to Eq. (17) with the numerical results using FEM for the orthotropic plate with free boundary conditions in Fig. 4. The differences between these two calculations are below 1.2 percent. These comparisons suggest that Eq. (17) can generally be used for orthotropic plates with a reasonably good accuracy.

From the computational view point, Eq. (17) provides a simple but sufficiently accurate formula to calculate the resonant frequencies of an orthotropic plate with [FFFF], [SSSS] and [CCCC] edges. Since these modal parameters are only dependent on \bar{S}_t and \bar{S}_r but not dependent on the physical properties and dimensions of the rectangular plate, we expect that the same formula can be used to compute the resonant frequencies for the orthotropic plate with [GGGG] edges. However, we need to determine a separate set of parameters for Q_ε , H_ε and J_ε in Eq. (17). Although it is possible to use the Rayleigh method again to derive the corresponding formula, we propose an alternative method to determine Q_ε , H_ε and J_ε . The method can then be generalized to more general boundary conditions in Section 4. Since these three parameters are the same for isotropic and orthotropic plates, we can simply substitute Eqs. (14a)–(14c) into Eq. (17) and re-write the resulting expression as

$$\bar{f}_{ij}^2 = \left(\frac{\pi^2}{4}\right) [(Q_i^4 R^2 + Q_j^4 R^{-2}) + 2J_i J_j + 2\nu(H_i H_j - J_i J_j)] \tag{21}$$

We can use, for example, the standard FEM program to compute the resonant frequencies of the isotropic plate by setting Poisson's ratio to zero and the aspect ratio varying from 1 to 4 at a step of 0.1. It is also of interest to note that f_{11} is zero for all aspect ratios which implies $Q_1 = J_1 = 0$. Next, a graph of \bar{f}_{ij}^2 is plotted versus $(R^2 + R^{-2})$ for $i = j = 2, 3, 4$ and 5, in turn. A straight line of different slopes and y-intercepts is obtained for different values of i and j . We can determine Q_ε from the slope and J_ε from the y-intercept of the graphs. Hence, we can show for [GGGG] that

$$Q_\varepsilon = \varepsilon - 1, \quad \text{for } \varepsilon \geq 1 \tag{22a}$$

$$J_\varepsilon = (\varepsilon - 1)^2, \quad \text{for } \varepsilon \geq 1. \tag{22b}$$

Table 1

Parametric values of Q_ε , H_ε and J_ε (where $\varepsilon = 1, 2, 3$) and β_Q , β_H and β_J (for $\varepsilon > 3$) for four common boundary conditions (free, simply supported, clamped and guides edges).

Type	ε	Q_ε	H_ε	J_ε
FFFF	1	0	0	0
	2	0	0	1.216
	3	1.506	1.248	5.017
	$\varepsilon > 3$	$\varepsilon + \beta_Q$, where $\beta_Q = -3/2$	$Q_\varepsilon^2(1 + \beta_H/Q_\varepsilon)$, where $\beta_H = -2/\pi$	$Q_\varepsilon^2(1 + \beta_J/Q_\varepsilon)$, where $\beta_J = 6/\pi$
SSSS	1	1	1	1
	2	2	4	4
	3	3	9	9
	$\varepsilon \geq 1$	$\varepsilon + \beta_Q$, where $\beta_Q = 0$	$Q_\varepsilon^2(1 + \beta_H/Q_\varepsilon)$, where $\beta_H = 0$	$H_\varepsilon = J_\varepsilon$
CCCC	1	1.506	1.248	1.248
	2	2.5	4.658	4.658
	3	3.5	10.02	10.02
	$\varepsilon > 1$	$\varepsilon + \beta_Q$, where $\beta_Q = 1/2$	$Q_\varepsilon^2(1 + \beta_H/Q_\varepsilon)$, where $\beta_H = -2/\pi$	$H_\varepsilon = J_\varepsilon$
GGGG	1	0	0	0
	2	1	1	1
	3	2	4	4
	$\varepsilon \geq 1$	$\varepsilon + \beta_Q$, where $\beta_Q = -1$	$Q_\varepsilon^2(1 + \beta_H/Q_\varepsilon)$, where $\beta_H = 0$	$H_\varepsilon = J_\varepsilon$

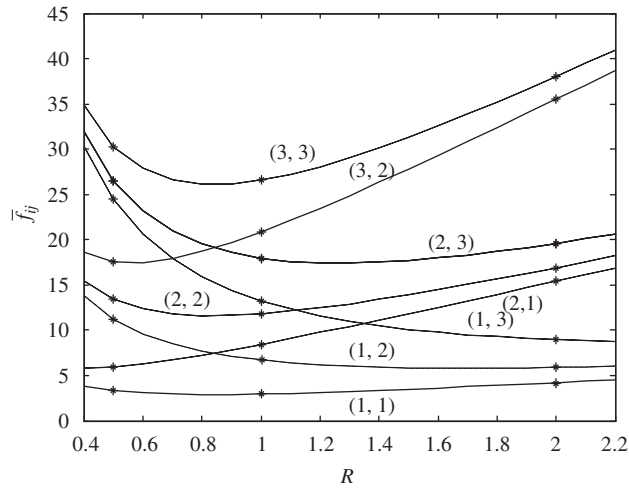


Fig. 2. The resonant frequencies of the simply supported orthotropic rectangular plates ($\bar{B}_k = 0.15\sqrt{2}$ and $\bar{B}_x/\bar{B}_y = 2$) calculated by the empirical formula and comparison with the results obtained from Sakata et al. [14] (*).

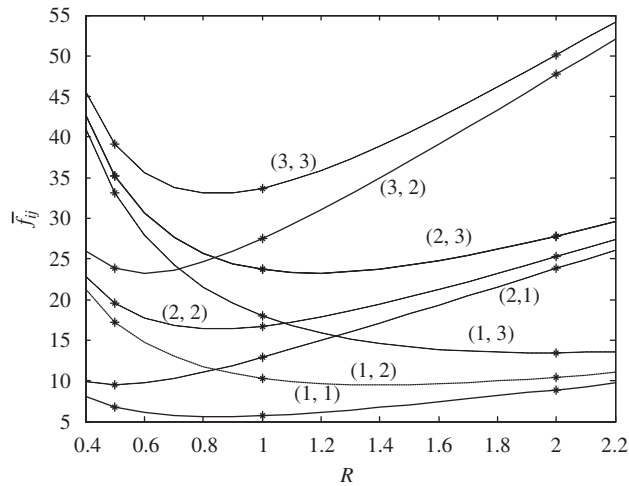


Fig. 3. The resonant frequencies of the clamped orthotropic rectangular plates ($\bar{B}_k = 0.15\sqrt{2}$ and $\bar{B}_x/\bar{B}_y = 2$) calculated by the approximate formula (solid line) and comparison with the results by Sakata et al. [14] (*).

Although other modal factors (i.e. different combinations of i and j) may be employed instead of those used above, the parametric values for Q_ε and J_ε remain very close to those given in Eqs. (22a) and (22b) above.

After the determination of Q_ε and J_ε , we can find H_ε as follows. The resonant frequencies are computed by setting R to 1 and varying Poisson's ratio from 0 to 0.9 for $i = j = 1, 2, 3$ and 4, in turn. A graph of \bar{f}_{ij}^2 is plotted against Poisson's ratio. The parametric value of H_ε can be determined from the slope of the graph. It is found that, the resonant frequencies are relatively independent on Poisson's ratio for a given pair of modal factor (i, j) . Hence, we have $H_i H_j - J_i J_j = 0$ which means

$$H_\varepsilon = J_\varepsilon = (\varepsilon - 1)^2. \tag{22c}$$

Indeed, this method has been applied to find the respective parametric values of Q_ε and J_ε for [FFFF], [SSSS] and [CCCC]. The numerical results are the same as those listed in Table 1. By using the method detailed above, it is reassuring to confirm that the analogous results are obtained comparable to the published formulas.

Dickinson [8] also obtained approximate formulas for other classical boundary conditions for [SSFF], [CCFF] and [CCSS]. If we follow the same procedures as discussed above, we can obtain an analogous formulas for [GGFF], [GGSS] and [GGCC]

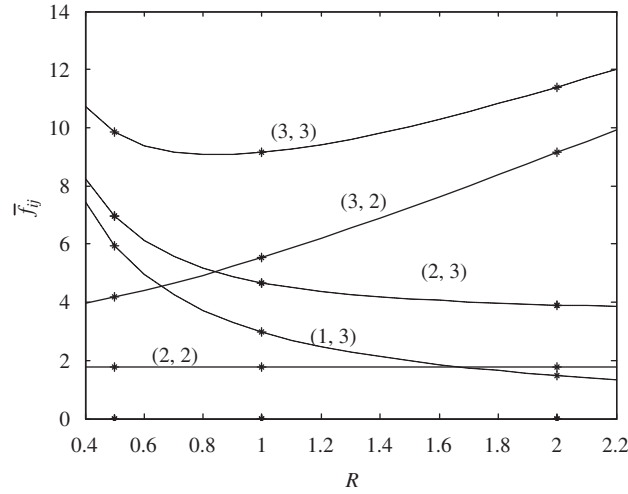


Fig. 4. The resonant frequencies of the free orthotropic rectangular plates ($\bar{B}_k = 0.15\sqrt{2}$ and $\bar{B}_x/\bar{B}_y = 2$) calculated by the approximate formula (solid line) and comparison with the results by FEM (*).

with $Q_\varepsilon, J_\varepsilon$ and H_ε given by

(i) [GGFF]

$$Q_\varepsilon = \varepsilon - 5/4, \quad \text{for } \varepsilon > 3 \tag{23a}$$

$$H_\varepsilon = (\varepsilon - 5/4)^2 \left[1 - \frac{1}{(\varepsilon - 5/4)\pi} \right], \quad \text{for } \varepsilon > 3 \tag{23b}$$

$$J_\varepsilon = (\varepsilon - 5/4)^2 \left[1 + \frac{3}{(\varepsilon - 5/4)\pi} \right], \quad \text{for } \varepsilon > 3. \tag{23c}$$

(ii) [GGSS]

$$Q_\varepsilon = \varepsilon - 1/2, \quad \text{for } \varepsilon \geq 1 \tag{24a}$$

$$H_\varepsilon = J_\varepsilon = (\varepsilon - 1/2)^2, \quad \text{for } \varepsilon \geq 1. \tag{24b}$$

(iii) [GGCC]

$$Q_\varepsilon = \varepsilon - 1/4, \quad \text{for } \varepsilon > 3 \tag{25a}$$

$$H_\varepsilon = J_\varepsilon = (\varepsilon - 1/4)^2 \left[1 - \frac{1}{(\varepsilon - 1/4)\pi} \right], \quad \text{for } \varepsilon > 3. \tag{25b}$$

The parameters for the boundary conditions of [GGGG], [GGFF], [GGSS] and [GGCC] are summarized in Table 2.

We test the accuracy of the empirical formula given in Eq. (17) for [GGGG], [GGFF], [GGSS] and [GGCC] with the appropriate parameters for $Q_\varepsilon, J_\varepsilon$ and H_ε derived earlier. In Fig. 5(a)–(d), we show typical plots of \bar{f}_{ij}^2 versus $(\bar{R}_{ij}^2 + \bar{R}_{ij}^{-2})$ for the orthotropic plate with the boundary supports of [GGGG], [GGFF], [GGSS] and [GGCC], respectively. Here, the numerical results for modes (2,2), (3,3), (4,4) and (5,5) with $\bar{B}_k = 0.15\sqrt{2}$ and $\bar{B}_x/\bar{B}_y = 2$ are shown. A set of calculations was conducted to confirm the accuracy for predicting the resonant frequencies of mode (1,1) by using Eq. (17). The numerical results for mode (1,1) are not shown in Fig. 5 for the clarity of presentation. It is because the natural frequencies for mode (1,1) are either zero or very small comparing to those of the other modes.

The discrepancies between these two numerical results are generally less than 2.4 percent. As predicted by Eq. (21), the term $(\bar{R}_{ij}^2 + \bar{R}_{ij}^{-2})$ varies linearly with the resonant frequencies. From the slopes of the y-intercepts, we can also confirm that Q_ε and J_ε for different boundary conditions are, indeed, given in Table 2.

Table 2

Parametric values of Q_ε , H_ε and J_ε (where $\varepsilon = 1, 2, 3$) and β_Q , β_H and β_J (for $\varepsilon > 3$) for the cases of [GGFF], [GGSS] and [GGCC].

Type	ε	Q_ε	H_ε	J_ε
GGFF	1	0	0	0
	2	0.752	0.3093	1.18
	3	1.7454	2.481	4.411
	$\varepsilon > 3$	$\varepsilon + \beta_Q$, where $\beta_Q = -5/4$	$Q_\varepsilon^2(1 + \beta_H/Q_\varepsilon)$, where $\beta_H = -1/\pi$	$Q_\varepsilon^2(1 + \beta_J/Q_\varepsilon)$, where $\beta_J = 3/\pi$
GGSS	1	0.5	0.25	0.25
	2	1.5	2.25	2.25
	3	2.5	6.25	6.25
	$\varepsilon \geq 1$	$\varepsilon + \beta_Q$, where $\beta_Q = -1/2$	$Q_\varepsilon^2(1 + \beta_H/Q_\varepsilon)$, where $\beta_H = 0$	$H_\varepsilon = J_\varepsilon$
GGCC	1	0.752	0.3093	0.3093
	2	1.749	2.481	2.481
	3	2.75	6.686	6.686
	$\varepsilon > 3$	$\varepsilon + \beta_Q$, where $\beta_Q = -1/4$	$Q_\varepsilon^2(1 + \beta_H/Q_\varepsilon)$, where $\beta_H = -1/\pi$	$H_\varepsilon = J_\varepsilon$

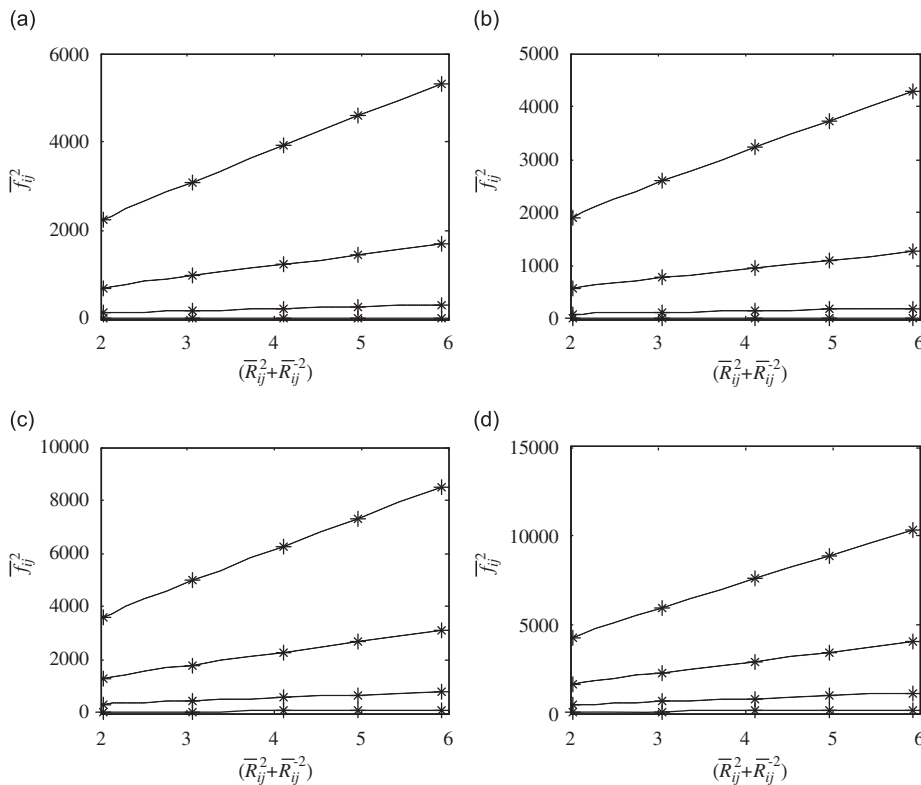


Fig. 5. The linear relationship of $(\bar{R}_{xy}^2 + \bar{R}_{xy}^{-2})$ in the function of \bar{f}_{ij}^2 for the orthotropic plate ($\bar{B}_k = 0.15\sqrt{2}$ and $\bar{B}_x/\bar{B}_y = 2$) with four classical boundary conditions: (a) [GGGG]; (b) [GGFF]; (c) [GGSS] and (d) [GGCC]. Solid line: mode (2,2); dash-dotted line: mode (3,3); dotted line: mode (4,4) and dashed line: mode (5,5). Numerical predictions according to the FEM are marked as "*" for different boundary conditions.

Next, we display the variation of \bar{f}_{ij}^2 with v_m for the same modes shown in Fig. 6(a)–(d). The numerical values for R , \bar{B}_k and \bar{B}_x/\bar{B}_y are chosen to be 1, $0.15\sqrt{2}$ and 2, respectively, in these plots. We can see from the figures that the slope of the straight line is zero for the range of v_m shown in the plots for [GGGG], which suggests that the predicted \bar{f}_{ij}^2 are independent on v_m , i.e. $H_\varepsilon = J_\varepsilon$ for all ε and for [GGFF], the term \bar{f}_{ij}^2 varies linearly with v_m . The numerical results are similar for other parameters and they are not shown for succinctness.

From the plots shown in Figs. 5 and 6, we can see that Eq. (17) offers a simple formula for predicting resonant frequencies of orthotropic and isotropic plates which are supported with guided edges. As expected, the predictions according to the empirical formula agree well with the FEM results (within the thickness of the lines). However, we only display five typical results calculated according to the FEM for each case. They are marked as * in Figs. 5 and 6.

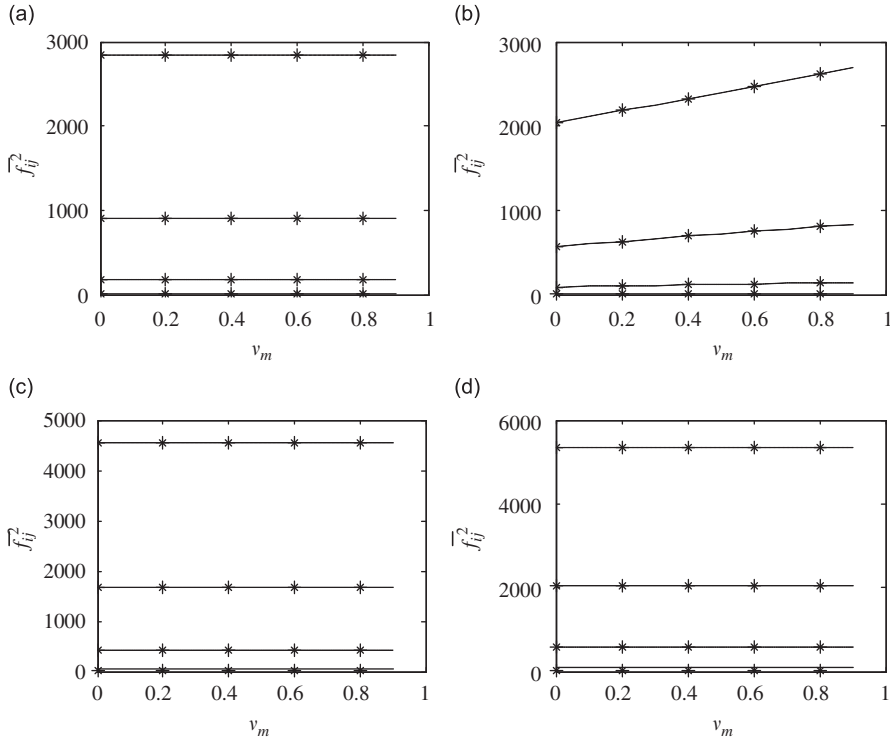


Fig. 6. The linear relationship of $\bar{\nu}$ in the function of \bar{f}_{ij}^2 for the orthotropic plate ($\bar{B}_k = 0.15\sqrt{2}$ and $\bar{B}_x/\bar{B}_y = 2$) with four classical boundary conditions: (a) [GGGG]; (b) [GGFF]; (c) [GGSS] and (d) [GGCC]. Solid line: mode (2,2); dash-dotted line: mode (3,3); dotted line: mode (4,4) and dashed line: mode (5,5). Numerical predictions according to the FEM are marked as “*” for different boundary conditions.

4. Approximate solutions for uniformly restrained edges for a square plate

A close examination of the boundary conditions, Eqs. (11a)–(11h), reveals that the non-dimensional spring constants [Eqs. (13a)–(13h)], are dependent on the aspect ratio, R , of the plate. They can be de-coupled from R when $L_x = L_y$, i.e. a square plate with $R = 1$. In this case, $Q_\varepsilon, J_\varepsilon$ and H_ε are only dependent on the non-dimensional spring constants defined in Eqs. (13a)–(13h). If the plate is supported by springs of uniform stiffness per unit length, then it is possible to derive empirical formulas for predicting the modal resonant frequencies of a square plate.

4.1. Edges with a variable rotational spring stiffness

A square plate is considered in our first test case where \bar{S}_r changes from 0 to ∞ but $\bar{S}_t(\rightarrow \infty)$ remains unchanged. In this case, the supports vary from [SSSS] to [CCCC]. It is remarkable that $H_\varepsilon = J_\varepsilon$ for all values of ε according to Table 1. We can then simplify Eq. (17) to

$$\bar{f}_{ij} = \frac{\pi}{2} \sqrt{(Q_i Q_j)^2 (\bar{R}_{ij}^2 + \bar{R}_{ij}^{-2}) + 2(\bar{B}_{xy} + \bar{B}_k) H_i H_j} \tag{26a}$$

because $H_i H_j - J_i J_j = 0$. Eq. (18) can then be reduced to

$$\bar{R}_{ij} = (E_x/E_y)^{1/4} (Q_i/Q_j), \tag{26b}$$

where R is set at 1 for a square plate. Furthermore, we can see that Q_ε and H_ε ($\varepsilon = i$ or j) are functions of \bar{S}_r only. A preliminary computational analysis has been conducted to determine the range for \bar{S}_r by using the standard FEM program. The numerical results have suggested that the edges can be treated effectively as [SSSS] if $\bar{S}_r \leq 10^{-2}$ and as [CCCC] if $\bar{S}_r > 10^5$.

The determination of the empirical functions for Q_ε and H_ε can be simplified considerably if we use $X_r \in (-2, 5)$ in favour of \bar{S}_r where

$$X_r = \log_{10}(\bar{S}_r). \tag{27}$$

We divide X_r into equal-spaced points from -2 to 5 with a step of 0.2 . For a given value of X_r , we can use the method described in Section 3 to determine β_Q and β_H . We then apply the method of Padé approximation [28] to approximate β_Q and β_H as follows:

$$\beta_Q(\bar{S}_r) \text{ or } \beta_H(\bar{S}_r) = \frac{\sum_{k=0}^n a_k X_r^k}{\sum_{k=1}^n b_k X_r^k}, \tag{28}$$

where a_k and b_k have different parameters for β_Q and β_H . We find that a fourth-order polynomial for the Padé approximants is sufficiently accurate to approximate the resonant frequencies of the square plate. Table 3 lists the coefficients of the polynomials for the rational functions. It is also noted that use of β_Q and β_H will not give an accurate prediction of the resonant frequencies for $\varepsilon = 1$. The problem can be traced back to the parameters used for calculating Q_1 and H_1 when $\bar{S}_r \rightarrow \infty$. In these two cases, $Q_1 = 1.506$ and $H_1 = 1.248$ should be used instead. By using the improved values for Q_1 and H_1 , we can derive the corresponding Padé approximants for $Q_1(\bar{S}_r)$ and $H_1(\bar{S}_r)$ with the forms also given in Eq. (28) but they are calculated with different sets of a_k and b_k . Numerical experiments suggest that use of fifth-order polynomials in the rational function leads to more accurate numerical results for these two cases. The parametric values for Q_1 and H_1 are also listed in Table 3 for ease of reference.

In a recent study, Nassar [15] derived an approximate formula of the fundamental frequency, $\bar{\lambda}_{11} = R\bar{f}_{11}/2\pi$, for an isotropic plate with $\alpha_r \in (0, \infty)$ and $\alpha_t \rightarrow \infty$ and different R . Gorman used the superposition method to obtain $\bar{\lambda}_{11}$ for the isotropic plate with different coefficients for the translational and rotational stiffness of the edges. We present their numerical results in terms of \bar{f}_{ij} and use them to validate the approximate formula derived in the present study. We only compare the numerical results with those taken from Nassar and Gorman [16] for the (1,1) mode only. We also compare with the numerical results obtained by the standard FEM program for modes (1,2), (2,2), (3,4) and (4,5). In all these numerical results, the aspect ratio of the isotropic rectangular plates is set at 1. Generally speaking, good agreements are obtained by using the corresponding Padé approximants for calculating $Q_\varepsilon(\bar{S}_r)$ and $H_\varepsilon(\bar{S}_r)$. These numerical values for $Q_\varepsilon(\bar{S}_r)$ and $H_\varepsilon(\bar{S}_r)$ are substituted into Eq. (26a) to calculate the resonant frequencies. The comparisons of the modal resonant frequencies are shown in Fig. 7. The average discrepancies between the empirical scheme and the standard FEM scheme are below 2.5 percent in all cases. For the fundamental modes, the average discrepancy between the numerical results obtained from the empirical scheme and those taken from Nassar and Gorman are below 1.5 percent.

Fig. 8 shows the comparison of the predicted resonant frequencies for the orthotropic plate. They are calculated by the empirical formula and by the standard FEM program. The average discrepancies between these two numerical results are well below 2.6 percent.

This approach can easily be extended for supports with other parametric values for the translational stiffness. For instance, if \bar{S}_t is taken as 1000, then the Padé approximants and their corresponding coefficients for the rational functions can be determined from the resonant frequencies obtained from the standard FEM results. The determined parameters are listed in Table 4 for completeness. For the case when $\varepsilon = 1$ and 2, we find that use of β_Q and β_H does not give satisfactory numerical results because more accurate values for Q_1, H_1, J_1, Q_2, H_2 and J_2 are needed when the translational stiffness gets smaller. In these situations, separate Padé approximants are required and these parametric values are listed in Table 4.

Using a_k and b_k in the approximate formula, we can calculate the corresponding modal frequencies \bar{f}_{ij} with the aspect ratio set at 1. We can compare these numerical results with those obtained from the FEM program for different modes. These comparisons are shown in Fig. 9 where the resonant frequencies of modes (1,1), (1,2), (2,2), (3,4) and (4,5) for the isotropic plates are chosen for the purpose of illustration. The average discrepancies of the predicted \bar{f}_{ij} between the two prediction schemes are well below 2.4 percent in all cases.

Table 3

Parametric values of $Q_\varepsilon, H_\varepsilon$ and J_ε (where $\varepsilon = 1, 2, 3$) and β_Q, β_H and β_J (for $\varepsilon > 3$) for the case of $\bar{S}_t \rightarrow \infty$ and $\bar{S}_r \in (10^{-2}, 10^5)$.

	a_0	a_1	a_2	a_3	a_4	a_5
β_Q	0.02639	0.03773	0.02416	0.008117	0.001159	0
$\beta_H = \beta_J$	-0.001692	-0.01134	-0.01855	-0.01183	-0.002594	0
Q_1	1.0872	-0.4243	0.4601	0.009575	0.009225	0
$H_1 = J_1$	0.9981	-0.9856	0.5114	-0.07316	0.01903	-0.002400
	b_0	b_1	b_2	b_3	b_4	b_5
β_Q	1	-0.7745	0.3436	-0.03034	0.005110	0
$\beta_H = \beta_J$	1	-0.8644	0.3379	-0.03127	0.007158	0
Q_1	1	-0.5381	0.3968	-0.008375	0.007026	0
$H_1 = J_1$	1	-0.9902	0.4993	-0.08075	0.01819	-0.002085

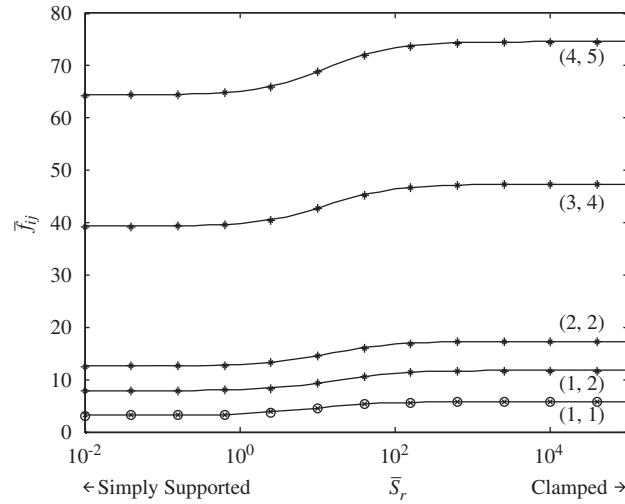


Fig. 7. Comparison of term \tilde{f}_{ij} of isotropic plates for the case of $\tilde{S}_t \rightarrow \infty$ and $\tilde{S}_r \in (10^{-2}, 10^5)$ calculated by approximate formula, Gorman [3] (\circ), Nassar [2] (\times) and FEM ($*$).

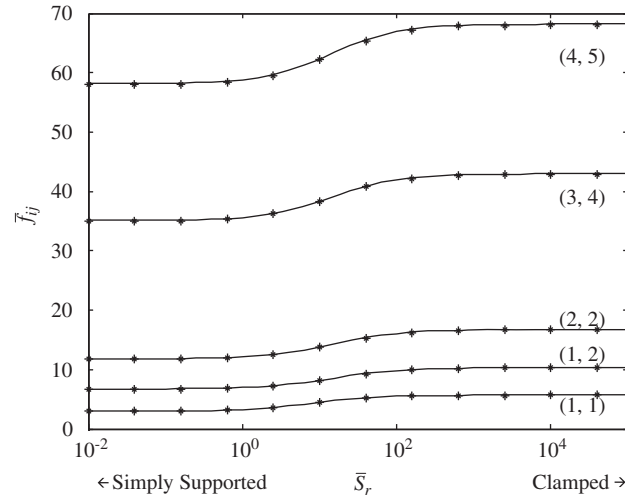


Fig. 8. Comparison of the resonant frequency \tilde{f}_{ij} of orthotropic rectangular plates ($\tilde{B}_k = 0.15\sqrt{2}$ and $\tilde{B}_x/\tilde{B}_y = 2$) for the case of $\tilde{S}_t \rightarrow \infty$ and $\tilde{S}_r \in (10^{-2}, 10^5)$ calculated by approximate formula and FEM ($*$).

4.2. Edges with variable translational stiffness

In this section, we wish to consider the case for a square plate where the edges change from [GGGG] to [CCCC], i.e. \tilde{S}_t varies from 0 to ∞ but $\tilde{S}_r(\rightarrow \infty)$ is kept constant. By examining the parametric values for Q_ε , H_ε and J_ε in Tables 1 and 2 for [CCCC] and [GGGG], we expect that $H_\varepsilon = J_\varepsilon$ as described in the last section. The approximate resonant frequency can also be computed by Eq. (26a) provided that Q_ε and H_ε are known. Again, we use Padé approximation to calculate $\beta_Q(\tilde{S}_t)$ and $\beta_H(\tilde{S}_t)$ which can then be used to approximate Q_ε and H_ε by applying Eqs. (19a) and (19b) for different ε . Prior numerical analyses indicate that the effective range for \tilde{S}_t is best set as $-1 \leq X_t \leq 6$ where

$$X_t = \log_{10}(\tilde{S}_t). \tag{29}$$

We can then calculate $\beta_Q(\tilde{S}_t)$ and $\beta_H(\tilde{S}_t)$ by using the following Padé approximations:

$$\beta_Q(\tilde{S}_t) \quad \text{or} \quad \beta_H(\tilde{S}_t) = \frac{\sum_{k=0}^n d_k X_t^k}{\sum_{k=0}^n d_k X_t^k}, \tag{30}$$

where up to fifth-order polynomials are needed to approximate these two functions. We also find that separate Padé approximants are needed to calculate Q_1 and H_1 , respectively, for better agreements with the FEM results. In Table 5, we list the corresponding parametric values for c_k and d_k used in Eq. (30) for information.

Table 4

Parametric values of Q_ε , H_ε and J_ε (where $\varepsilon = 1, 2, 3$) and β_Q , β_H and β_J (for $\varepsilon > 3$) for the case of $\bar{S}_t = 1000$ and $\bar{S}_r \in (10^{-2}, 10^5)$.

	a_0	a_1	a_2	a_3	a_4	a_5
β_Q	-0.4661	0.1783	-0.1760	-0.01311	0	0
$\beta_H = \beta_J$	0.02473	-0.03275	-0.006754	-0.004343	0	0
Q_1	1.0190	-0.3347	0.4652	0.03454	0.01346	0
$H_1 = J_1$	0.9431	-0.4716	0.3912	0.05484	0.01860	0
Q_2	1.9001	-1.0748	0.8180	0.01975	0.02429	0
$H_2 = J_2$	2.6775	-3.0383	1.7491	-0.3203	0.1751	-0.01207
	b_0	b_1	b_2	b_3	b_4	b_5
β_Q	1	-0.3990	0.3723	0.02636	0	0
$\beta_H = \beta_J$	1	-0.5765	0.3747	0.03976	0	0
Q_1	1	-0.4433	0.4303	0.01698	0.01124	0
$H_1 = J_1$	1	-0.6391	0.3459	0.01579	0.01195	0
Q_2	1	-0.5870	0.4249	0.006520	0.01224	0
$H_2 = J_2$	1	-1.0769	0.6210	-0.1313	0.05987	-0.004141

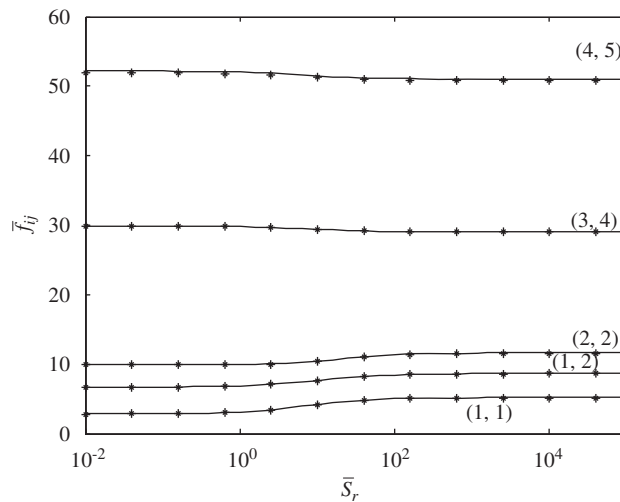


Fig. 9. Comparison of the resonant frequency \bar{f}_{ij} of isotropic plates for the case of $\bar{S}_t = 1000$ and $\bar{S}_r \in (10^{-2}, 10^5)$ calculated by approximate formula (solid line) and FEM (*).

Table 5

Parametric values of Q_ε , H_ε and J_ε (where $\varepsilon = 1, 2, 3$) and β_Q , β_H and β_J (for $\varepsilon > 3$) for the case of $\bar{S}_t \rightarrow \infty$ and $\bar{S}_r \in (10^{-1}, 10^6)$.

	c_0	c_1	c_2	c_3	c_4	c_5
β_Q	-0.9981	0.5840	-0.1123	0.007991	0	0
$\beta_H = \beta_J$	0.01341	0.01164	-0.002187	-0.001765	0.003178	-7.883×10^{-4}
Q_1	0.2387	-0.06369	-0.008337	0.004859	-5.667×10^{-4}	5.694×10^{-4}
$H_1 = J_1$	0.1261	0.009590	-0.01123	-0.001729	-1.211×10^{-4}	7.899×10^{-4}
	d_0	d_1	d_2	d_3	d_4	d_5
β_Q	1	-0.5811	0.1156	-0.006028	0	0
$\beta_H = \beta_J$	1	-1.4368	0.8543	-0.2372	0.02668	-3.495×10^{-4}
Q_1	1	-0.9074	0.3592	-0.07450	0.007923	2.458×10^{-5}
$H_1 = J_1$	1	-1.0847	0.5012	-0.1176	0.01288	6.221×10^{-5}

Based on Eq. (30), we can calculate the modal frequencies for the present situation with $\bar{S}_t \in (0, \infty)$ and $\bar{S}_r \rightarrow \infty$ by using the parametric values listed in Table 5. As shown in Fig. 10, we compare the results of the resonant frequencies for the isotropic plates calculated according to the empirical formula and the standard FEM program for modes (1,1), (1,2), (2,2), (3,4) and (4,5) with R set at 1. The differences between these two numerical results are within 2.7 percent.

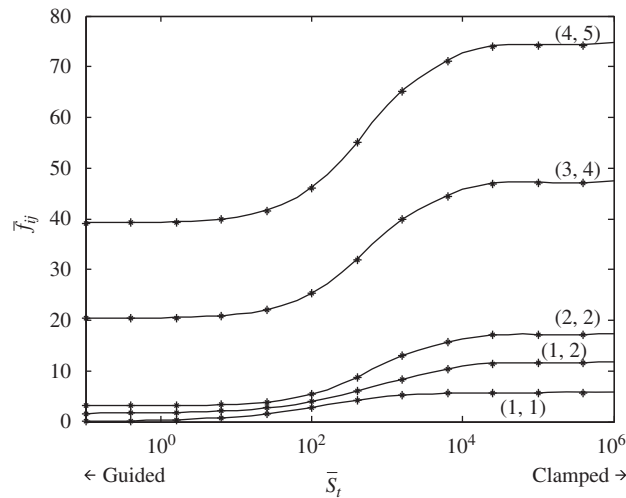


Fig. 10. Comparison of the resonant frequency \bar{f}_{ij} of isotropic plates for the case of $\bar{S}_r \rightarrow \infty$ and $\bar{S}_r \in (10^{-1}, 10^6)$ calculated by approximate formula (solid line) and FEM (*).

5. Conclusions

Approximate formulas have been developed for calculating the resonant frequencies of the vibration of orthotropic/isotropic rectangular plates with edges mounting with arbitrarily elastic translational and rotational restraints. The solutions are given in closed forms for general cases of uniform restraints on all edges. The empirical formulas are suitable for both isotropic and orthotropic plates and they are explicit in terms of the restraint parameters, elastic properties and geometric ratio of the plate. The calculated results are compared with the published results and the numerical results calculated according to the standard FEM program. The discrepancies in predicting the resonant frequencies are around 1.5 percent for the lower elastic modes and around 2.5 percent for the higher modes.

The empirical formulas derived herein is simple to implement even an elementary calculator may be used to calculate the resonant frequencies of an orthotropic, rectangular plate supported at its edges with the classical boundary conditions. On the other hand, Padé approximants have been developed to compute the corresponding resonant frequencies with general boundary conditions. Again, an elementary calculator may be used to compute the resonant frequencies with no prior knowledge of vibration and plate theory. Although the study only shows three examples with general boundary conditions, the method can be easily extended to other situations.

Acknowledgements

The project is supported in part by the Federal Aviation Administration (FAA) under Contract/Grant no. 07-C-NE-PU. This FAA project is monitored by Bill He. Any opinions, findings and conclusions or recommendations expressed in this material are those of the authors and do not necessarily reflect the views of the FAA, NASA or Transport Canada.

References

- [1] D. Young, Vibration of rectangular plates by the Ritz method, *Journal of Applied Mechanics* 17 (1950) 448–453.
- [2] R.F.S. Hearmon, The frequency of flexural vibration of rectangular orthotropic plates with clamped or supported edges, *Journal of Applied Mechanics* 26 (1959) 537–540.
- [3] G.B. Warburton, The vibrations of rectangular plates, *Proceedings of the Institution of Mechanical Engineers, Series A* 168 (1954) 371–384.
- [4] G.B. Warburton, Response using the Rayleigh–Ritz method, *Journal of Earthquake Engineering and Structural Dynamics* 7 (1979).
- [5] G.B. Warburton, S.L. Edney, Vibration of rectangular plates with elastically restrained edges, *Journal of Sound and Vibration* 95 (1984) 537–552.
- [6] A.W. Leissa, Vibration of plates, National Aeronautics and Space Administration Report, SP-160, 1969.
- [7] A.W. Leissa, The free vibration of rectangular plates, *Journal of Sound and Vibration* 31 (1973) 257–293.
- [8] S.M. Dickinson, The buckling and frequency of flexural vibration of the rectangular isotropic and orthotropic plates using Rayleigh's method, *Journal of Sound and Vibration* 61 (1978) 1–8.
- [9] S.M. Dickinson, E.K.H. Li, On the use of simply supported plate functions in the Rayleigh–Ritz method applied to the vibration of rectangular plates, *Journal of Sound and Vibration* 82 (1982) 292–297.
- [10] P.A.A. Laura, R.O.G. Grossi, Transverse vibrations of rectangular anisotropic plates with edges elastically restrained against rotation, *Journal of Sound and Vibration* 64 (1979) 257–267.
- [11] P.A.A. Laura, R.O.G. Grossi, Transverse vibrations of rectangular plates with edges elastically restrained against translation and rotation, *Journal of Sound and Vibration* 75 (1981) 101–107.
- [12] P.A.A. Laura, Comments on natural frequencies of rectangular plates using a set of static beam functions in the Rayleigh–Ritz method, *Journal of Sound and Vibration* 200 (1997) 540–542.

- [13] R.B. Bhat, Natural frequencies of rectangular plates using characteristic orthogonal polynomials in the Rayleigh–Ritz method, *Journal of Applied Mechanics* 102 (1985) 493–499.
- [14] T. Sakata, K. Takahashi, R.B. Bhat, Natural frequencies of orthotropic rectangular plates obtained by iterative reduction of the partial differential equation, *Journal of Sound and Vibration* 189 (1996) 89–101.
- [15] E.M. Nassar, Rapid calculation of the resonance frequency for the rotationally restrained rectangular plates, *American Institute of Aeronautics and Astronautics Journal* 17 (1979) 6–11.
- [16] D.J. Gorman, A general solution for the free vibration of rectangular plates resting on uniform elastic edge supports, *Journal of Sound and Vibration* 139 (1990) 325–335.
- [17] D.J. Gorman, A general solution for the free vibration of rectangular plates with arbitrarily distributed lateral and rotational elastic edge support, *Journal of Sound and Vibration* 174 (1994) 451–459.
- [18] D.J. Gorman, Free vibration analysis of Mindlin plates with uniform elastic edge support by the superposition method, *Journal of Sound and Vibration* 207 (1997) 335–350.
- [19] D. Zhou, Natural frequencies of elastically restrained plates using a set of statics of beam functions in the Rayleigh–Ritz method, *Computers and Structures* 57 (1995) 731–735.
- [20] D. Zhou, Natural frequencies of rectangular plates using a set of statics of beam functions in the Rayleigh–Ritz method, *Journal of Sound and Vibration* 189 (1996) 81–88.
- [21] P. Cupial, Calculation of the natural frequencies of composite plates by the Rayleigh–Ritz method with orthogonal polynomials, *Journal of Sound and Vibration* 201 (1997) 385–387.
- [22] W.L. Li, Vibration analysis of rectangular plates with general elastic boundary supports, *Journal of Sound and Vibration* 273 (2004) 619–635.
- [23] W.L. Li, Vibroacoustic analysis of rectangular plates with elastic rotational edge restraints, *Journal of the Acoustical Society of America* 120 (2006) 769–779.
- [24] W.L. Li, X. Zhang, J. Du, Z. Liu, An exact series solution for the transverse vibration of rectangular plate with general elastic boundary supports, *Journal of Sound and Vibration* 321 (2009) 254–269.
- [25] R.D. Blevins, *Formulas for Natural Frequency and Mode Shape*, Van Nostrand Reinhold, New York, 1979.
- [26] W. Soedel, *Vibrations of Shells and Plates*, Marcel Dekker, New York, 1993.
- [27] J.N. Reddy, *Theory and Analysis of Elastic Plates and Shells*, second ed., CRC Press, Taylor & Francis, New York, 2007.
- [28] W.H. Press, S.A. Teukolsky, W.T. Vetterling, B.R. Flannery, *Numerical Recipes in FORTRAN: The Art of Computing*, second ed., Cambridge University Press, 1992, p. 194.